

# Thermal and Structural Analysis of Heparin-PEO-PDMS-PEO-Heparin Pentablock Copolymers

YONG JOO KIM,<sup>1</sup> YONG KIEL SUNG,<sup>1</sup> AI ZHI PIAO,<sup>2</sup> DAVID W. GRAINGER,<sup>2,\*</sup> TERUO OKANO,<sup>2,†</sup> and SUNG WAN KIM<sup>2,‡</sup>

<sup>1</sup>Department of Chemistry, College of Sciences, Dongguk University, Seoul 100-715, South Korea;

<sup>2</sup>Center for Controlled Chemical Delivery, University of Utah, Salt Lake City, Utah 84112

## SYNOPSIS

ABCBA-type amphiphilic block copolymers comprising polydimethylsiloxane (PDMS), poly(ethylene oxide) (PEO), and heparin segments were synthesized by coupling reactions between end-functionalized oligomers. These multiblock copolymers were characterized to examine bulk properties using <sup>1</sup>H-NMR, FTIR, end-group analysis, and sulfur elemental analysis. Block copolymers were further characterized in bulk using differential scanning calorimetry and X-ray diffraction measurements. The PDMS glass transition remains unchanged with increasing PEO content, indicating coexistence of pure PDMS with mixed phases. Furthermore, endothermic melting of the block copolymers shifts to higher temperatures and becomes more intense with increasing PEO molecular weight. Additionally, the crystallinity of the PEO segment in the block copolymers increases with increasing PEO molecular weight. The PEO melting endotherm peak shifts from near 318 to 323 K with annealing. In the cooling thermogram, the block copolymers exhibit two crystallization exotherms, one near 303 K and the other near 193 K, attributed to PEO and PDMS recrystallization and nucleation, respectively. © 1994 John Wiley & Sons, Inc.

## INTRODUCTION

Many block copolymer systems exhibit two-phase morphology, consistent with nonideal intra- and interpolymer segmental interactions. Because of their segmented construction and covalent bonds between chemically distinct blocks, block copolymers exhibit immiscibility and morphological properties manifested on a micro- rather than macroscale dimension typical of incompatible physical blends.<sup>1</sup> This is due to the influence of the intersegment linkage that restricts the extent to which incompatible phases can separate. Nevertheless, the thermal properties of block copolymers resemble those of physical blends. They display multiple thermal transitions,

such as glass transitions and/or crystalline melting points, characteristic of each component.<sup>2</sup> By contrast, random copolymers display a single, homogeneous phase with a respective, compositionally dependent glass transition temperature. Furthermore, although crystallinity is possible in block systems due to long sequences, it is diminished or eliminated in the random copolymer systems due to a disruption of chain regularity. Because of differing chemistries in each block, segments are often not completely compatible in a thermodynamic sense, resulting in varying degrees of phase separation in the solid state.

Amphiphilic copolymers composed of hydrophilic and hydrophobic blocks have demonstrated unique bulk and surface properties and interfacial behaviors.<sup>3-10</sup> Polymeric hydrophilic/hydrophobic micro-phase-separated structures have been proposed<sup>4</sup> as a key parameter for controlling the interfacial reactivity between polymers and blood as they are reported to inhibit both protein deposition and platelet aggregation. Additionally, several polymer surfaces have been modified with the natural glycosamino-

\* To whom correspondence should be addressed.

† Current address: Tokyo Women's Medical College, 8-1 Kawada-cho, Shinjuku-bu, Tokyo 162, Japan.

‡ Current address: Department of Chemistry, Colorado State University, Ft. Collins, CO 80523.

Journal of Applied Polymer Science, Vol. 54, 1863-1872 (1994)

© 1994 John Wiley & Sons, Inc.

CCC 0021-8995/94/121863-10

glycan bipolymer, heparin, in order to inhibit surface induced clotting.<sup>11-15</sup> Hydrophilic spacer groups have also been used to extend immobilized heparin away from surfaces to enhance its interaction with coagulation factors.<sup>16-20</sup>

Block copolymer strategies have incorporated hydrophobic polymer blocks connected to heparin via hydrophilic copolymer blocks.<sup>5-10</sup> Vulic et al.<sup>5</sup> reported the synthesis of ABC-type block copolymers containing a heparin block, a hydrophilic poly(ethylene oxide) block, and a hydrophobic polystyrene block and also characterized their blood compatibility. Recently, Sung et al.<sup>6</sup> reported the bulk and surface characteristics of biocompatible PDMS-PEO-heparin multiblock copolymers. Other work<sup>7-10</sup> has described the synthesis, characterization, and surface properties of amphiphilic ABC and ABCBA-type block copolymers containing PDMS, PEO, and heparin. Silicone polymers have shown significant and widespread success as biomaterials in implant and pharmaceutical applications.<sup>21</sup> PEO has also received much attention as a potential biomaterial with unique, biocompatible properties.<sup>22</sup> By attaching these polymers linearly as block copolymers, the aim of these efforts was to provide a blood-compatible, heparinized coating to improve the bulk and surface properties of existing polymer substrates. Much of the surface and interfacial properties of these novel polymer materials has been studied.<sup>8-10</sup> Not only was heparin detected at the surface of these copolymer films,<sup>8-10</sup> but heparin was found to be bioactive using in both *in vitro*<sup>8,9</sup> and *in vivo* assays<sup>8,20</sup> using serum and whole blood. Nevertheless, the bulk properties of these amphiphilic heparin-containing block copolymers have not yet been studied in significant detail.

In this work, we describe the further characterization of ABCBA-type amphiphilic block copolymers containing PDMS, PEO, and bioactive heparin segments. The glass transition temperature, crystalline melting characteristics, annealing effects, and cold crystallization of the block copolymers were determined by differential scanning calorimetry. Assessment of block copolymer crystallinity was also determined using X-ray powder diffraction.

## EXPERIMENTAL

### Synthesis of Multiblock Copolymers

$\alpha,\omega$ -Di[heparin-PEO-DMS pentablock copolymers [PDMS(PEO-Hep)<sub>2</sub>] were synthesized via a coupling reaction of the triblock copolymer precursor

PDMS(PEO-NH<sub>2</sub>)<sub>2</sub> with derivatized heparin<sup>8</sup> by a similar procedure as used for fabricating the ABC triblock copolymer, PDMS-PEO-Hep.<sup>7</sup> For these experiments, diamino-terminated PEO with molecular weights of 2000 (PEO2), 4000 (PEO4), and 6000 (PEO6) (Jeffamines, Texaco) were coupled to PDMS(TDI)<sub>2</sub> in separate reactions. PDMS(TDI)<sub>2</sub> was prepared by adding PDMS(NH<sub>2</sub>)<sub>2</sub> (Petrarch-Hüls) (15% w/v in toluene) dropwise to a solution of toluene diisocyanate (TDI, 2% w/v in toluene), and a final ratio of [NH<sub>2</sub>]/[NCO] = 0.5 was obtained. PDMS(PEO-NH<sub>2</sub>)<sub>2</sub> block copolymers were synthesized by adding the PDMS(TDI)<sub>2</sub> toluene solution to  $\alpha,\omega$ -diamino PEO (15% w/v in toluene) until the final ratio of [NH<sub>2</sub>]/[NCO] was 2.4. All reactions were stirred under nitrogen for several days. Unreacted PDMS(NH<sub>2</sub>)<sub>2</sub> and PEO(NH<sub>2</sub>)<sub>2</sub> were removed by washing reaction products with a 10-fold excess mixture of ether and hexane (3 : 7 v/v) for 12 h and a 10-fold excess of water for 24 h. To increase heparin solubility in organic media, commercial heparin was subjected to cation exchange with benzyltrimethylammonium bromide to yield the triton-B form with one aldehyde group per molecule.<sup>7,8</sup> This heparin form was coupled to PDMS(PEO-NH<sub>2</sub>)<sub>2</sub> block copolymers by reductive amination using sodium cyanoborohydride.<sup>7,8</sup>

### Identification of Block Copolymers

Infrared spectra of both prepolymers and block copolymers were obtained from films cast on sodium chloride cells using a Nicolet 5-MX FTIR spectrophotometer. Proton NMR spectra were obtained from samples in chloroform-*d*<sub>1</sub> using a JEOL PMX instrument (90 MHz). Amino group functionalization for the PDMS and PEO prepolymers as well as the PDMS(PEO-NH<sub>2</sub>)<sub>2</sub> copolymers was analyzed by potentiometric titration.<sup>7,8</sup> Sulfur elemental analysis was obtained on a Lecox Corp. Model SC1321IR analyzer.

### Thermal Characterization of Block Copolymers

A Perkin-Elmer DSC-4 equipped with a TADS computer was used for differential scanning calorimetry measurements (DSC) to measure  $T_g$  and  $T_m$ . Calibration was most conveniently carried out by melting a carefully weighed sample of very pure reference material, usually semiconductor-grade indium. Samples of 5-10 mg were measured over a range of temperature from 123 to 423 K under helium at a scanning rate of 20°/min. For annealing thermograms, sealed aluminum pans were annealed

in the DSC cell for 20 min at 323 K and then rapidly quenched to 123 K. DSC scans were taken after quenching with each sample being used only once. For cooling thermograms, the DSC cell was heated to 323 K (above the highest DSC endotherm temperature exhibited by the samples). DSC scans taken were recorded immediately during cooling at a scanning rate of 20°/min.

### X-ray Characterization

X-ray powder diffraction profiles were recorded for copolymer solid samples using a  $\text{CuK}\alpha$  beam ( $\lambda = 1.54 \text{ \AA}$ ) in an X-ray diffractometer (Rigaku D-MAX IIIB).

## RESULTS AND DISCUSSION

### Identification of Multiblock Copolymers

The IR spectra of  $\text{PDMS}(\text{NH}_2)_2$ ,  $\text{PDMS}(\text{TDI})_2$ , and  $\text{PEO}(\text{NH}_2)_2$  are shown in Figure 1. Telechelic isocyanated PDMS was prepared from the telechelic diamine-terminated PDMS oligomer using TDI in solution coupling reactions.<sup>8</sup> IR vibrational bands characteristic of urea bond formation are indicated by the presence of N—H stretch at  $3320 \text{ cm}^{-1}$ , amide I at  $1645 \text{ cm}^{-1}$ , and amide II at  $1540 \text{ cm}^{-1}$  as shown in Figure 1(B). These peaks were unique to

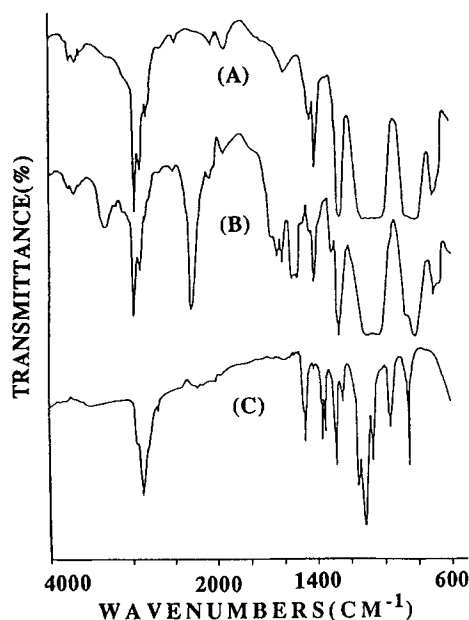


**Figure 1** FTIR spectra for (A)  $\text{PDMS}(\text{NH}_2)_2$ , (B)  $\text{PDMS}(\text{TDI})_2$ , and (C)  $\text{PEO}(\text{NH}_2)_2$ .

products from TDI functionalization and were not present in simple mixtures of the PDMS and diisocyanates. A strong adsorption at  $2270 \text{ cm}^{-1}$  is characteristic of free isocyanate groups. The FTIR spectra of the triblock and heparinized pentablock copolymers are also shown in Figure 2(A) and (B), respectively. When isocyanated PDMS prepolymers were coupled to amino telechelic PEO, FTIR spectra demonstrated new N—H stretching absorbance bands at  $3520$  and  $3380 \text{ cm}^{-1}$ , and the prominent isocyanate peak disappeared, indicating the formation of urea linkages between PDMS and PEO in two different chemical environments.

Proton NMR spectra for PEO, PDMS, and the  $\text{PDMS}(\text{PEO-NH}_2)_2$  block copolymer are shown in Figure 3. Methyl proton resonance signals of the siloxane backbone at 0.1 ppm and the methylene resonance of PEO at 3.4–3.8 ppm are shown. Signal integration confirms the proper ratio of protons in the block copolymer constituents as listed in Table I. NMR integral ratios indicate that the desired coupling reactions have been accomplished in the anticipated stoichiometry. In addition, end-group analysis, also shown in Table I, demonstrates the presence of functional amino groups in all steps of the synthetic process. This supports the assertion that the desired stoichiometric products are obtained. Elemental analysis shows that pure heparin contains 6.1% sulfur by weight, whereas the sulfur content of  $\text{PDMS}(\text{PEO-Hep})_2$  was 1.3% by weight, indicating that heparin comprises 21.3% (w/w) of the heparinized block copolymers. This result confirms that heparin is coupled into each block copolymer chain at a ratio of 2 : 1, providing additional, consistent evidence for ABCBA-type pentablock copolymer formation.

### DSC Thermograms of Block Copolymers

DSC results for the triblock copolymers, the heparinized pentablock copolymers, and pure oligomer samples of PEO, PDMS, and heparin are summarized in Table II. Glass transition temperatures were chosen as the intersection of the curve tangent line and the upper base line, a point near the onset of heat capacity change through the transition region. The melting temperature,  $T_m$ , and the crystallization temperature,  $T_c$ , were defined as the extrapolated onset points. According to the nomenclature for differential thermal analysis curves,<sup>23</sup> the extrapolated onset is best defined as the point of transition because the point of intersection gives the most reproducible value experimentally independent of the operator.

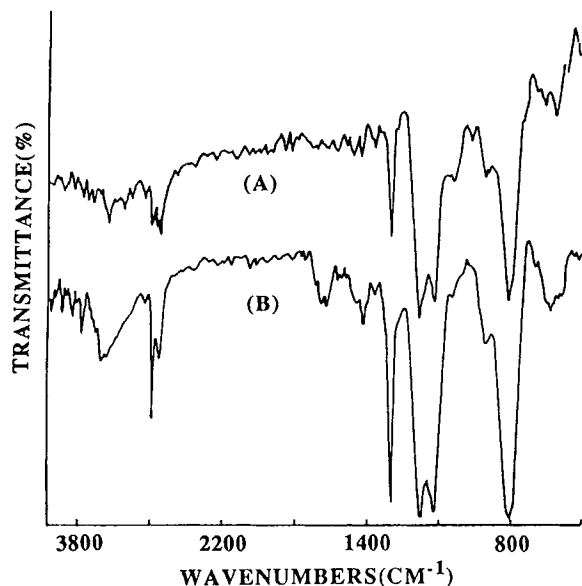


**Figure 2** FTIR spectra for block copolymers (A) PDMS(PEO-NH<sub>2</sub>)<sub>2</sub> and (B) PDMS(PEO-Hep)<sub>2</sub>.

Pure PEO shows a  $T_g$  at 232 K and a  $T_m$  at about 323 K. The crystalline melting temperature location is consistent with that found by others.<sup>24,25</sup> Pure PDMS shows a  $T_g$  at 150 K, a crystalline transition for PDMS at 183 K, and a melting peak of crystalline of PDMS at 223 K.<sup>26,27</sup> Heparin displays a large exo-

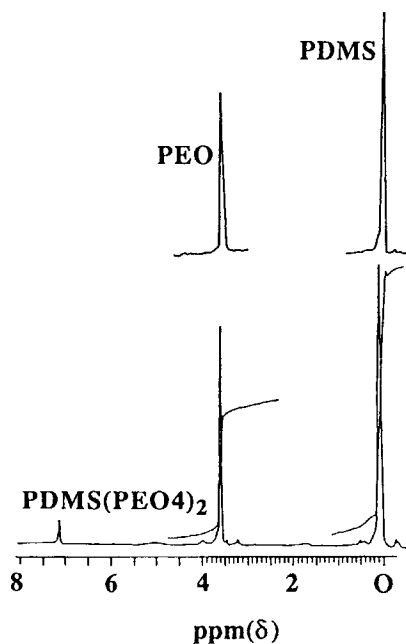


**Figure 3** <sup>1</sup>H-NMR spectra for PDMS, PEO, and the PDMS(PEO-NH<sub>2</sub>)<sub>2</sub> triblock copolymer.

**Table I** Composition and End-group Concentrations in Block Copolymers

Polymer	PEO (mol %) <sup>a</sup>	Mole Ratio <sup>b</sup>		Amino Groups (mol/g × 10 <sup>-5</sup> )
		PEO	PDMS	
PDMS(PEO2) <sub>2</sub>	10.2	1	4.5	4.38
PDMS(PEO4) <sub>2</sub>	20.5	1	1.9	4.14
PDMS(PEO6) <sub>2</sub>	30.7	1	1.3	1.26

<sup>a</sup> In feed.

<sup>b</sup> By <sup>1</sup>H-NMR integration.

thermic peak at 523 K due either to thermal degradation or recrystallization.<sup>10</sup> As shown Figure 4, DSC thermograms of the complete ABCBA block copolymers shows well-defined thermal transitions that are easily identified as follows: glass transition for PDMS at approximately 150 K; crystalline transition for PDMS at 170 K; melting transition for crystalline PDMS at 220 K; and an endothermic peak related to the melting of the crystalline PEO fraction ranging from 310 to 320 K. The  $T_m$  of PEO in the nonheparinized triblock copolymers is consistently shifted to lower temperatures compared to pure PEO, indicating a small degree of phase mixing with PDMS (data not shown). The  $T_m$  of PEO in these heparinized block copolymers is also shifted slightly to 310–315 K, indicating a small degree of miscibility of the PEO with other blocks in the ABCBA system. These data suggest that the copolymers are semicrystalline materials characterized by the coexistence of distinct segregated chemically homogeneous domains. Surprisingly, both PEO and PDMS segments maintain significant crystallinity in copolymer samples.

Glass transition temperatures for polymers depend strongly on thermal history, internal stresses present, side chains, molecular weight, and chemical structure. Glass transition temperatures for the PDMS segment in triblock and heparinized pentablock copolymers are represented in Figure 5 and Table II. Very little shift in the PDMS  $T_g$  with various coupled components is observed, suggesting that amorphous PDMS segments are unaffected by block copolymers with different PDMS and PEO compositions, i.e., noncrystalline PDMS appears to be unaffected by the presence of PEO or heparin segments. However, PDMS cold crystallization temperatures are influenced by the incorporation of PEO and heparin into the copolymer. As further described below, crystalline PDMS phases appear to undergo alterations as PEO content and chain length changes. This indicates at least three types

**Table II Thermal Analysis of PEO and PDMS in the Block Copolymers**

Polymer	PEO		PDMS					Heparin Exotherm (K)
	$T_m$ (K)	$\Delta H_m$ (J/g)	$T_g$ (K)	$T_c$ (K)	$T_m$ (K)	$\Delta H_c$ (J/g)	$\Delta H_m$ (J/g)	
PEO4	323.2	146.2	—	—	—	—	—	—
PDMS	—	—	150.0	183.0	223.0	-8.6	19.4	—
Heparin	—	—	—	—	—	—	—	523
PDMS(PEO2) <sub>2</sub>	306.5	31.5	148.9	188.0	219.6	-6.3	17.6	—
PDMS(PEO4) <sub>2</sub>	318.0	47.0	148.9	171.7	215.1	-8.4	8.8	—
PDMS(PEO6) <sub>2</sub>	319.6	42.0	149.9	169.3	217.4	-7.2	11.3	—
PDMS(PEO2-Hep) <sub>2</sub>	308.7	6.7	150.8	167.7	219.6	-6.3	17.6	547
PDMS(PEO4-Hep) <sub>2</sub>	311.6	21.8	151.2	170.2	219.2	-7.9	12.6	543
PDMS(PEO6-Hep) <sub>2</sub>	315.8	28.1	150.9	169.3	216.6	-5.5	10.1	523

of PDMS phases: pure amorphous, pure crystalline, and a mixed amorphous phase with PEO. PEO crystallinity, which would necessarily exclude PDMS, is known to increase with its molecular weight. Crystalline fractions for PEO blocks in copolymers analyzed here (shown in Table III) support this trend and will be discussed further below.

#### Annealing Effects and Cooling Thermograms

Annealing proved experimentally inaccessible in block copolymers having a  $T_m$  above 343 K because of their poor thermal stability. However, these block copolymers could be first heated for 20 min to 323 K and then studied using the calorimetric methods described above. Annealing results for PEO and PDMS in the triblock and the heparinized pentablock copolymers are shown in Figure 6 over tem-

perature ranges relevant to PEO and PDMS transitions. Lower temperature transitions observed for the PDMS  $T_g$  and  $T_c$  at 150–170 K have disappeared with annealing. The PEO  $T_m$  peak shifts from near 318 K in the initial thermogram toward its pure  $T_m$  of 323 K with annealing. The initial, low  $T_m$  for PEO in this unannealed system suggests that PEO is initially quite phase-mixed. It is difficult to discern directly whether PEO is mixed predominantly with heparin or PDMS. However, based on the thermal shifts seen for both triblock and heparinized block copolymers in Figure 6, phase-mixed regions of both PEO-heparin and PEO-PDMS with a larger portion of PDMS-PEO are likely present. The appearance of thermal transitions associated with pure PDMS and PEO phases as well as for phase-mixed regions of these constituents supports the contention that

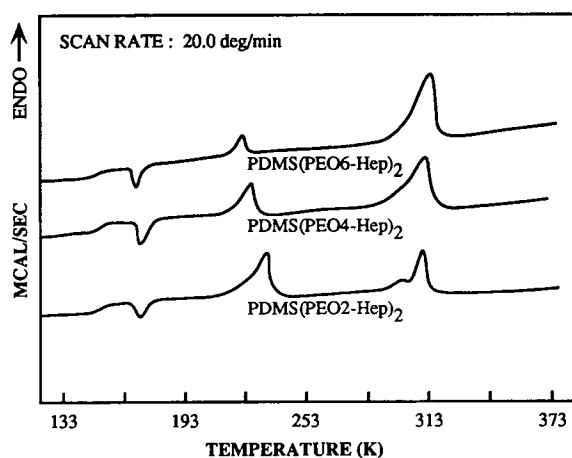


**Figure 4** DSC thermograms for heparinized pentablock copolymers.

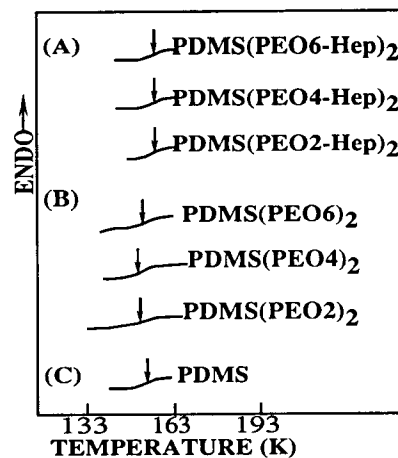


**Figure 5** Glass transition temperature in PDMS segments in (A) triblock and (B) heparinized pentablock copolymers.

**Table III Crystalline Fractions and Enthalpies of Melting of PEO in the Block Copolymers**

Polymer	$\Delta H_m$ (J/g)	PEO Cry. (%) <sup>a</sup>
PDMS(PEO2) <sub>2</sub>	31.5	16
PDMS(PEO4) <sub>2</sub>	47.0	24
PDMS(PEO6) <sub>2</sub>	42.0	22
PDMS(PEO2-Hep) <sub>2</sub>	6.7	3
PDMS(PEO4-Hep) <sub>2</sub>	21.8	11
PDMS(PEO6-Hep) <sub>2</sub>	28.1	14

<sup>a</sup> Weight fraction of PEO in copolymer that is crystalline  $\times 100$ , i.e., wt crystalline PEO/total PEO  $\times 100$ .

the heparinized block copolymer is phase-separated to a certain extent after annealing with associated areas of phase mixing.

Triblock and heparinized block copolymers show varied thermal behaviors after a melt recrystallization cycle. Since thermal behavior for the block

copolymers involves not only polymer melting characteristics, but also its crystallization, it is compelling to consider the characteristics of the sample under precisely controlled cooling conditions. Cooling results for both triblock and heparinized pentablock copolymers are shown in Figure 7. The data illustrate the crystallization behavior (exotherms) for two different types of crystalline phases in both triblock and the heparinized block copolymers. These copolymers exhibit two crystallization exotherms, one near 303 K attributed to PEO and the other near 193 K due to PDMS cold crystallization.<sup>26,27</sup>

### PEO Segment Melting Point Depression

Melting in crystalline polymers typically occurs over a finite range of temperatures. This phenomenon results from the fact that most crystalline polymers are not entirely crystalline and contain regions of crystallites surrounded by amorphous fractions.

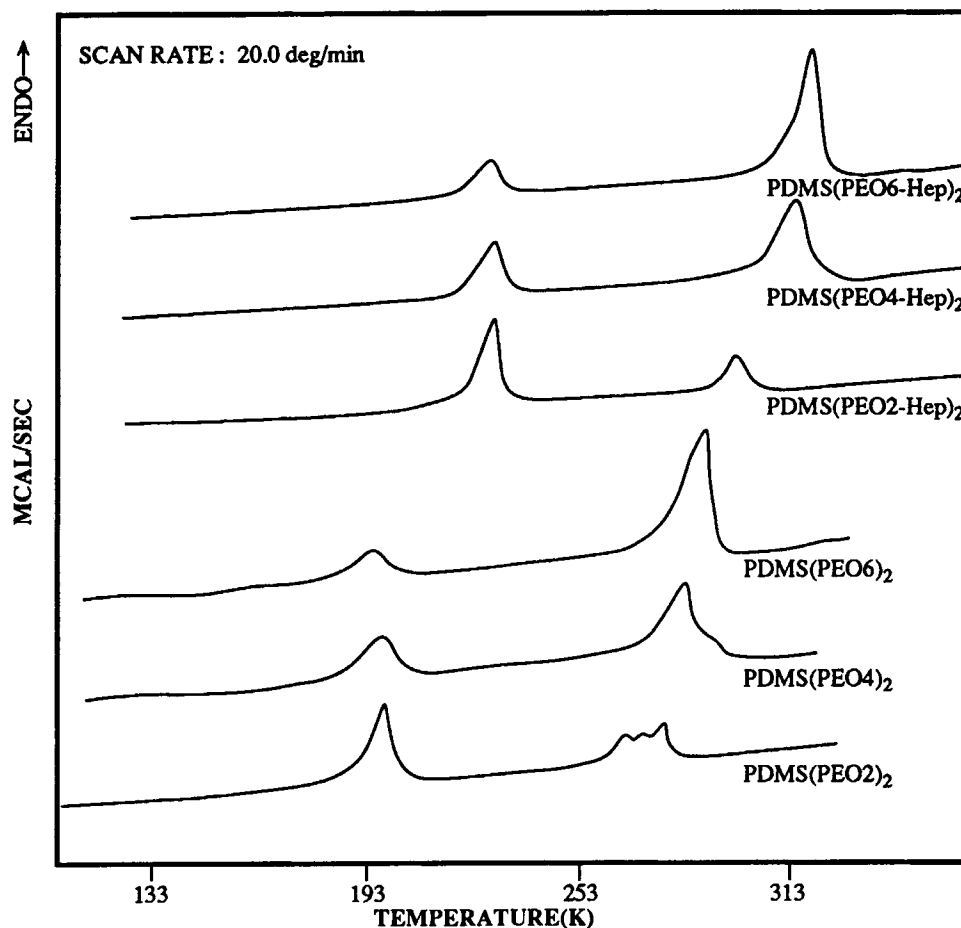


**Figure 6** Annealing thermograms for triblock and heparinized pentablock copolymers.

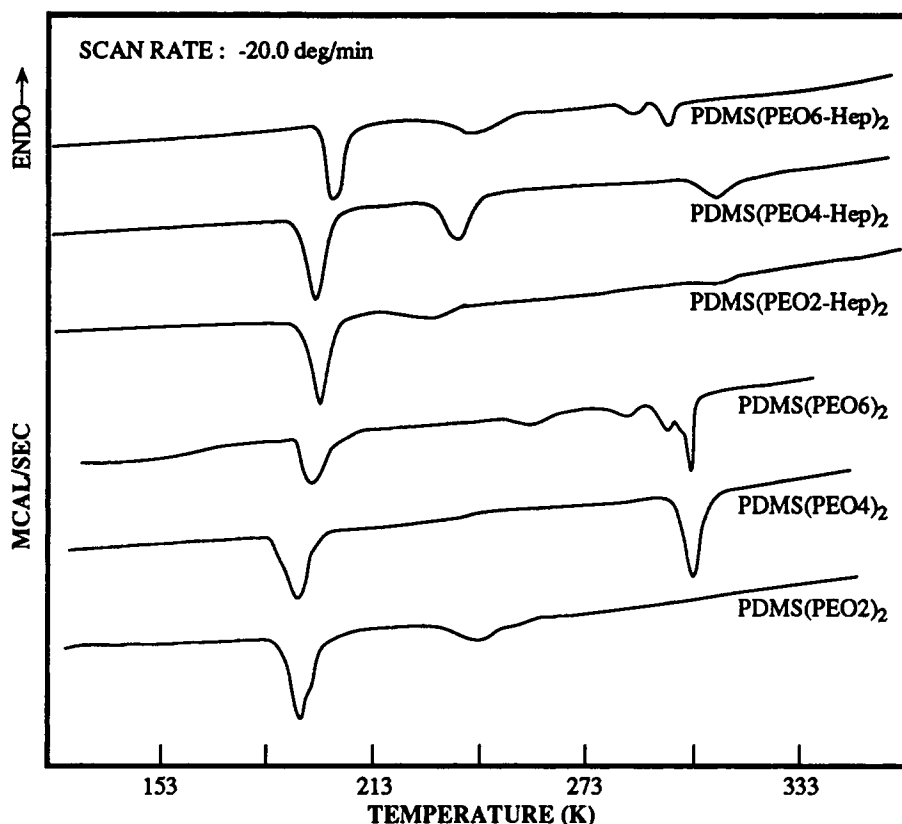


Figure 7 Cooling thermograms for triblock and heparinized pentablock copolymers.

Depending on the amorphous:crystalline ratios, different melting temperatures are recorded. Enthalpic values of melting for PEO in both the triblock and heparinized pentablock copolymers vs. temperature as derived from DSC thermograms are also summarized in Table II. In agreement with others,<sup>28</sup> their endothermic melting points shift to higher temperature ranges and become larger with increasing PEO molecular weight. Plots of PEO molecular weight vs.  $T_m$  for the PEO, triblock copolymers, and heparinized pentablock copolymers are shown in Figure 8.

Melting point trends in these systems are interesting: From a theoretical standpoint, melting points should not fluctuate and should be independent of block composition if the crystalline block is large enough and if the system is at thermal equilibrium.<sup>29</sup> Given the various crystalline and amorphous contents in the block copolymers, progressive shifts in melting point peaks with PEO content may be explained using Flory's polymer diluent theory.<sup>30</sup> Lower melt points for crystalline PEO fractions and subsequent varying levels of miscibility may be caused in part by differing degrees of phase mixing<sup>31</sup> of PEO with amorphous PDMS phases or by dif-

ferent forms of PEO crystals in the block copolymers and heparinized block copolymers.<sup>32</sup> Other systems<sup>33</sup> comparing polymer-diluent mixtures demonstrate melt peak shifts that can be modeled by Flory's theory correlating  $T_m$  to thermodynamic interaction

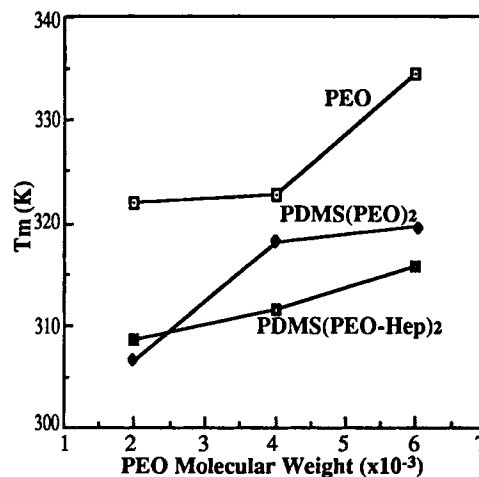


Figure 8 PEO melting point vs. PEO molecular weight in triblock and heparinized pentablock copolymers.

parameters and volume fractions of each phase.<sup>28</sup> Phase mixing of PEO and PDMS probably accounts for the peak shifts in  $T_m$  as well as differing degrees of crystalline fraction in each case. The increasing amorphous PDMS content likely induces increasing levels of phase mixing, leading to crystalline imperfections that cause melting point depressions.

### Degrees of Crystallinity for PEO Segments

Calorimetric summation of different melt temperatures and relative populations of crystallites bearing these  $T_m$  will result in broadening of observed calorimetric peaks. Crystallite size and amorphous fraction, in turn, are functions of branching, chain length, and molecular weight distribution as well as of thermal history.<sup>34</sup> Enthalpy changes associated with PEO's first-order melt transition, calculated as a ratio of DSC peak areas, are well characterized and reproducible by comparing the peak area of the endothermic peak with that of pure indium. A plot of PEO molecular weight vs.  $\Delta H_m$  for PEO, triblock, and heparinized pentablock copolymers is shown in Figure 9. The linear relationship in both triblock and heparinized pentablock copolymers supports a correlation between PEO molecular weight and the peak shift. Assuming that the Gibbs free energy change during a phase transition is nearly zero (equilibrium), the entropy of the transition can be calculated from the known data of  $\Delta H$  and melting temperature:

$$\Delta G_m = \Delta H_m - T_m \cdot \Delta S_m, \Delta G \cong 0 \quad (1)$$

$$\Delta S_m = \Delta H_m/T_m \quad (2)$$

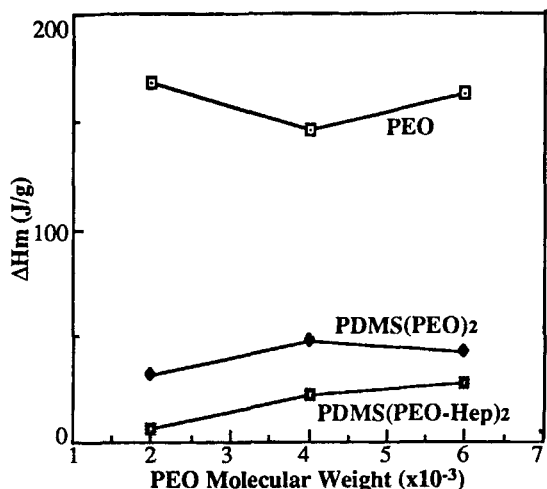


**Figure 9** PEO melting enthalpy vs. PEO molecular weight in triblock and heparinized pentablock copolymers.

Table II shows the  $T_m$  derived from DSC thermogram peaks and the  $\Delta H_m$  obtained from peak areas.  $\Delta S_m$  is calculated from  $\Delta H_m$  and  $T_m$  by this method for both PEO and PDMS segments.  $\Delta H_m$  values for PEO and PDMS segments in the copolymers are both less than those measured for pure PEO and PDMS, respectively, and these  $\Delta H_m$  values for pure phases are lower than those reported for higher molecular weight analogs.<sup>35</sup> This likely reflects differences in crystalline fractions as a function of molecular weight (see below). Additionally,  $\Delta H_m$  values for these segments are inversely correlated: For a given sample, low  $\Delta H_m$  values for PEO segments are consistently associated with relatively high values of  $\Delta H_m$  for PDMS segments. For the heparin-containing samples,  $\Delta H_m$  values for PEO segments increase with PEO molecular weights, whereas those for PDMS decrease accordingly. These trends may indicate mutual effects of PEO and PDMS segment crystallization within these copolymers where one segment (e.g., PEO) creates a crystallized phase of high  $\Delta H_m$  compelling the other phase (e.g., PDMS) to reduce its crystalline fraction (and  $\Delta H_m$ ) during solidification.  $\Delta S_m$  for PEO values of the triblock and heparinized pentablock copolymers increase with increasing PEO molecular weight. A plot of PEO molecular weight vs.  $\Delta S_m$  for the PEO, triblock, and heparinized pentablock copolymers is shown in Figure 10.

The enthalpy of melting,  $\Delta H_m$ , can be used to calculate the degree of crystallinity ( $\chi_c$ ) for related unknown polymer samples if a sample of 100% crystalline phase is used as a reference. The degree of crystallinity,  $\chi_c$ , was calculated by the following equation<sup>36</sup>:

$$\chi_c = \Delta H_m / \Delta H_m^0 \quad (3)$$

where  $\Delta H_m$  is derived from DSC thermograms as described above and  $\Delta H_m^0$  is the enthalpy change of melting for a 100% crystalline sample standard. Calculations of  $\chi_c$  for PEO according to PEO molecular weight in the block copolymers are shown in Table III. Degrees of crystallinity for PEO phases were calculated from the experimentally determined enthalpy of fusion and a value of 194 J/g for  $\Delta H_m^0$  derived for 100% crystalline PEO.<sup>22,25,27,28</sup> Weight fractions of crystalline PEO increase with increasing PEO molecular weight in the block copolymers.

### X-ray Diffraction

X-ray diffraction methods allow determination of the relative amounts of crystalline and amorphous



material in a sample if it is possible to resolve the contributions of the two types of structures in the X-ray diffraction pattern. X-ray powder diffraction patterns used to investigate crystallinity for PEO, heparin, and block copolymers are shown in Figure 11. The first main reflection for pure PEO ( $19^\circ$ ) is very sharp and corresponds to an intermolecular spacing between PEO linear chains of 4.6 Å. This PEO reflection is also observed in the block copolymers as well but peaks are broadened and diminished, indicating structural perturbations. Diffraction patterns for triblock and heparinized pentablock copolymers have reflections at the same position as that for pure PEO, which become broader as the amount of PDMS increases. Apparently, in this case, phase immiscibility diminishes PEO crystallinity, supporting thermal analysis results.

Tri- and pentablock copolymers exhibit a common, broad reflection ( $12^\circ$ ), corresponding to a chain spacing of 7.3 Å. This peak is absent in both the pure heparin and PEO samples, implying that it might be attributed to the PDMS phase. Previous scattering work<sup>27</sup> has shown an interchain spacing of 9.0 Å for pure silicone polymer networks.

## CONCLUSIONS

ABCBA-type amphiphilic block copolymers were synthesized via coupling reactions of PDMS(PEO-NH<sub>2</sub>)<sub>2</sub> with derivatized heparin. <sup>1</sup>H-NMR results, FTIR spectra, and end-group and sulfur elemental analyses are all consistent with the synthesis of ABCBA pentablock copolymers. These samples were

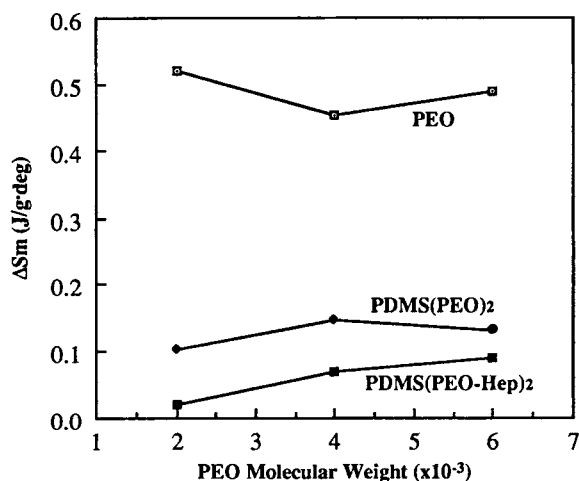


**Figure 10** PEO melting entropy vs. PEO molecular weight in triblock and heparinized pentablock copolymers.

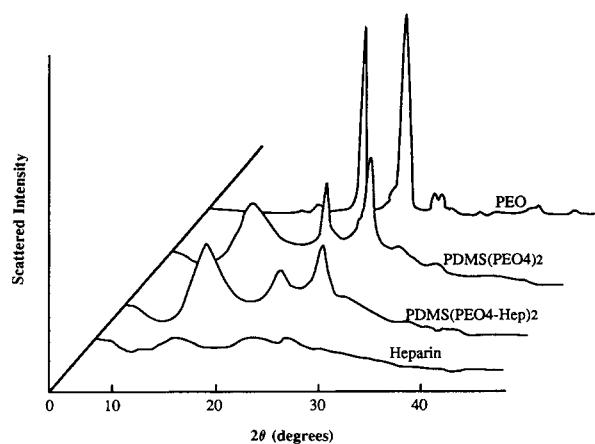


**Figure 11** X-ray powder diffraction profiles for PEO, heparin, and block copolymers.

characterized in bulk by differential scanning calorimetry and X-ray diffraction.

The block copolymers were found to be semi-crystalline materials characterized by the coexistence of different segregated domains and segment aggregation states. The thermal data are consistent with multiple aggregation states for both PDMS and PEO in the copolymers that change with PEO chain length (and, hence, with PEO content). PDMS and PEO exist in pure isolated immiscible phases (microphase-separated domains) that coexist with a miscible PDMS-PEO mixed-phase fraction. As discussed below, PEO in its pure state is at least partially crystalline, whereas when mixed with PDMS, it is certainly much more amorphous. Block copolymer endothermic melting points shift to higher temperature and increase with increasing PEO molecular weight. Crystallinity of PEO in the block copolymer also increases with increasing PEO molecular weight. The PEO  $T_m$  peak shows shifts from near 318 K in the initial thermogram toward its pure  $T_m$  of 323 K with annealing. In the cooling thermogram, the block copolymers exhibit two PEO crystallization exotherms, characteristic of PEO and PDMS, respectively.

We thank Dr. Geoff Russell for helpful comments regarding calorimetry and Prof. Jan Feijen (Twente University, The Netherlands) for inspiring ideas regarding heparinized copolymers. D.W.G. was a recipient of a Pharmaceutical Manufacturer's Association Predoctoral Fellowship.

## REFERENCES

1. M. Matsuo and S. Sagaye, in *Colloidal and Morphological Behavior of Block Copolymers*, G. E. Molau, Ed., Plenum Press, New York, 1977.

2. B. Ke, *Newer Methods of Polymer Characterization*, Wiley-Interscience, New York, 1964.
3. T. Okano, M. Shimada, T. Aoyagi, I. Shinohara, K. Kataoka, K. Abe, and Y. Sakurai, *J. Biomed. Mater. Res.*, **20**, 919 (1986).
4. T. Okano, M. Urumo, N. Sugiyama, M. Shimada, I. Shinohara, K. Kataoka, and Y. Sakurai, *J. Biomed. Mater. Res.*, **20**, 1035 (1986).
5. I. Vulic, T. Okano, S. W. Kim, and J. Feijen, *J. Polym. Sci. A*, **26**, 381 (1988).
6. Y. K. Sung, D. W. Grainger, T. Okano, J. Feijen, and S. W. Kim, in *IUPAC International Symposium on Macromolecules Preprints*, 1988, p. 588.
7. D. W. Grainger, J. Feijen, and S. W. Kim, *J. Biomed. Mater. Res.*, **22**, 231 (1988).
8. A. Z. Piao, C. Nojiri, K. D. Park, H. Jacobs, J. Feijen, and S. W. Kim, *J. Biomater. Sci. Polym. Ed.*, **1**, 299 (1990).
9. D. W. Grainger, K. Knutson, T. Okano, and S. W. Kim, *J. Biomed. Mater. Res.*, **24**, 403 (1990).
10. D. W. Grainger, T. Okano, S. W. Kim, Y. K. Sung, D. Briggs, D. G. Castner, and B. D. Ratner, *J. Biomed. Mater. Res.*, **24**, 547 (1990).
11. M. F. A. Goosen and M. V. Sefton, *J. Biomed. Mater. Res.*, **17**, 359-374 (1983).
12. P. Heyman, C. S. Cho, J. C. McRae, D. B. Olsen, and S. W. Kim, *J. Biomed. Mater. Res.*, **19**, 419-436 (1985).
13. C. Fougnot, D. Labarre, M. C. Boffa, J. Jozefowicz, and M. Jozefowicz, in *Macromolecular Biomaterials*, G. W. Hastings and P. Ducheyne, Eds., CRC Press, Boca Raton, FL, 1984, pp. 217-238.
14. S. W. Kim and J. Feijen, in *CRC Crit. Rev. Biocompat.*, **1**(3), 229-260 (1985).
15. J. E. Wilson, *Plast. Techn. Eng.*, **16**, 119-208 (1981).
16. D. E. Gregonis, D. E. Buerger, R. A. van Wagnen, and J. D. Andrade, *Trans. Soc. Biomater.*, **7**, 766-772 (1984).
17. Y. Mori, S. Nagaoka, H. Takaguchi, N. Noguchi, H. Tanzawa, and Y. Soishiki, *Trans. Am. Soc. Artif. Inter. Organs*, **27**, 459-468 (1982).
18. E. W. Merrill and E. W. Salzman, *ASAIO J.*, **6**, 60-65 (1983).
19. K. D. Park, T. Okano, C. Nojiri, and S. W. Kim, *J. Biomed. Mater. Res.*, **22**, 977-992 (1988).
20. C. Nojiri, K. D. Park, D. W. Grainger, H. A. Jacobs, T. Okano, H. Koyanagi, and S. W. Kim, *Trans. Am. Soc. Artif. Inter. Organs*, **36**, M168 (1990).
21. T. Davanthan, J. E. Sluetz, and K. A. Young, *Biomater. Med. Dev. Art. Org.*, **8**, 4 (1980).
22. J. M. Harris, Ed., *Poly(ethylene glycol) Chemistry*, Plenum Press, New York, 1992.
23. G. Lombardi, in *International Confederation for Thermal Analysis*, 1977.
24. X. Li and S. L. Hsu, *J. Polym. Sci. B Polym. Phys. Ed.*, **22**, 1331 (1984).
25. Y. Kambe, *Polym. Rep.*, **32**, 3861 (1980).
26. C. L. Lee, O. K. Johannson, O. L. Flanigan, and P. Hahn, *Polym. Prepr. Am. Chem. Soc. Div. Polym. Chem.*, 1311 (1969).
27. S. J. Clarson, K. Dodgson, and J. A. Semlyer, *Polymer*, **26**, 930 (1985).
28. C. Price, K. A. Evans, and C. Booth, *Polymer*, **16**, 196 (1975).
29. P. J. Flory, *Principles of Polymer Chemistry*, Cornell University Press, Ithaca, NY, 1953.
30. L. Mandelkern, *J. Appl. Phys.*, **26**, 443 (1955).
31. I. A. Katine, M. S. Anasagasti, M. C. Peleteiro, and R. Valenciano, *Eur. Polym. J.*, **23**, 907 (1987).
32. D. R. Beech, C. Booth, C. J. Picles, R. R. Sharpe, and J. R. S. Waring, *Polymer*, **13**, 246 (1972).
33. B. Ke, *J. Polym. Sci.*, **50**, 79 (1961).
34. E. B. Manche and B. Carroll, in *Physical Methods in Macromolecular Chemistry*, B. Carroll, Ed., Marcel Dekker, New York, 1972, Vol. 2.
35. J. Brandup and E. H. Immergut, Eds., *Polymer Handbook*, 2nd ed., Wiley-Interscience, New York, 1975.
36. M. Dole, *J. Polym. Sci.*, **186**, 57 (1967).
37. Y. K. Ovchinnikov, G. S. Markova, and V. A. Kargin, *Vysokomol. Soyed.*, **A11**, 329 (1969).

Received January 10, 1994

Accepted May 4, 1994